Acta Tropica 146 (2015) 141–151

Contents lists available at ScienceDirect

Acta Tropica

journal homepage: www.elsevier.com/locate/actatropica

Biochemical and molecular characterization of the calcineurin in *Echinococcus granulosus* larval stages☆

María Celeste Nicolao[a,b], Andrea C. Cumino[a,b,c,*]

[a] *Laboratorio de Zoonosis Parasitarias, Departamento de Biología, Facultad de Ciencias Exactas y Naturales, Universidad Nacional de Mar del Plata (UNMdP), Funes 3350, Nivel Cero, 7600 Mar del Plata, Argentina*
[b] *Consejo Nacional de Investigaciones Científicas y Técnicas (CONICET), Argentina*
[c] *Departamento de Química, Facultad de Ciencias Exactas y Naturales, Universidad Nacional de Mar del Plata (UNMdP), Funes 3350, Nivel 2, 7600 Mar del Plata, Argentina*

ARTICLE INFO

Article history:
Received 10 October 2014
Received in revised form 6 March 2015
Accepted 10 March 2015
Available online 25 March 2015

Keywords:
Echinococcus
Calcineurin
Cyclosporine-A
Calcium chelators
Larval development

ABSTRACT

Calcineurin (CaN) is a Ca^{2+}-calmodulin activated serine–threonine protein phosphatase that couples the local or global calcium signals, thus controlling important cellular functions in physiological and developmental processes. The aim of this study was to characterize CaN in *Echinococcus granulosus* (Eg-CaN), a human cestode parasite of clinical importance, both functionally and molecularly. We found that the catalytic subunit isoforms have predicted sequences of 613 and 557 amino acids and are substantially similar to those of the human counterpart, except for the C-terminal end. We also found that the regulatory subunit consists of 169 amino acids which are 87% identical to the human ortholog. We cloned a cDNA encoding for one of the two catalytic subunit isoforms of CaN (Eg-can-A1) as well as the only copy of the Eg-can-B gene, both constitutively transcribed in all *Echinococcus* larval stages and responsible for generating a functionally active heterodimer. Eg-CaN native enzyme has phosphatase activity, which is enhanced by Ca^{2+}/Ni^{2+} and reduced by cyclosporine A and Ca^{2+} chelators. Participation of Eg-CaN in exocytosis was demonstrated using the FM4-64 probe and Eg-CaN-A was immunolocalized in the cytoplasm of tegumental cells, suckers and excretory bladder of protoscoleces. We also showed that the Eg-can-B transcripts were down-regulated in response to low Ca^{2+} intracellular level, in agreement with decreased enzyme activity. Confocal microscopy revealed a striking pattern of Eg-CaN-A in discrete fluorescent spots in the protoscolex posterior bladder and vesicularized protoscoleces beginning the vesicular differentiation. In contrast, Eg-CaN-A was undetectable during the pre-microcyst closing stage while a high DDX-like RNA helicase expression was evidenced. Finally, we identified and analyzed the expression of CaN-related endogenous regulators.

1. Introduction

Calcineurin (CaN), also known as protein phosphatase 2B (PP2B), is a Ca^{2+}-calmodulin activated serine–threonine protein phosphatase involved in different signaling pathways (Rusnak and Mertz, 2000). CaN plays a key role in the coupling of local or global calcium signals that control immediate cellular responses and modify gene transcription. CaN is a heterodimer composed of a catalytic A subunit (CaN-A) and a Ca^{2+}-binding regulatory B subunit (CaN-B). CaN-A contains a catalytic phosphatase domain and a regulatory domain which includes a CaN-B binding domain, a calmodulin (CaM)-binding domain and an autoinhibitory domain, which binds to the catalytic site in the absence of Ca^{+2}/CaM, thus inhibiting PP2B activity. CaN, encoded by one or more genes for each subunit, is considered an evolutionarily conserved protein in all eukaryotes (Rusnak and Mertz, 2000).

The biological functions of CaN, which involve Ca^{2+}-dependent cellular events, have been studied in many organisms, including mammals, plants, fungi, invertebrates and protozoa. When compared to other protein phosphatases (Sim et al., 2003), CaN interacts with a limited number of substrates, such as proteins involved in membrane trafficking and cytoskeletal association, ion channels, targeting and regulatory proteins and transcription factors (Rusnak

☆ Nucleotide sequence data reported in this paper are available in the GenBank database under GenBank Accession Number KC146906 (Eg-*can*-A1), HQ454284 (Eg-*can*-B) and KC146907 (Eg-*chp*).

* Corresponding author at: Laboratorio de Zoonosis Parasitarias, Departamento de Biología, Facultad de Ciencias Exactas y Naturales, Universidad Nacional de Mar del Plata (UNMdP), Funes 3350, Nivel Cero, 7600 Mar del Plata, Argentina.
Tel.: +54 223 4752426x450.
E-mail address: acumino@mdp.edu.ar (A.C. Cumino).

http://dx.doi.org/10.1016/j.actatropica.2015.03.016
0001-706X/

and Mertz, 2000; Li et al., 2011). Consequently, CaN encompasses the transcriptional regulation in connection with Ca^{2+} signaling in the immune, nervous, vascular, musculoskeletal and endocrine systems and controls important cell functions in physiological and developmental processes (Aramburu et al., 2004). In vertebrate secretory cells, such as neurons and immune system and pancreatic acinar cells, CaN regulates endocytosis–exocytosis through dephosphorylation of dynamin, synaptotagmin, dephosphins, actin and kinesin (Sim et al., 2003; Grybko et al., 2007; Bennett et al., 2010).

In fungi and in invertebrates, CaN has been associated with growth and developmental regulation (Chen et al., 2010; Aramburu et al., 2004; Bandyopadhyay et al., 2004), whereas in protozoan parasites it has been linked to the regulation of the life cycle, development and exocytosis, thus becoming a promising target for the development of inhibitors that block invasion and limit parasite growth (Rascher et al., 1998; Banerjee et al., 1999; Orrego et al., 2014; Singh et al., 2014). In helminth parasites, such as *Hymenolepsis microstoma*, *H. diminuta* and *Schistosoma mansoni*, it has been proved that CaN is involved in ion homeostasis (Roberts et al., 1997; Mecozzi et al., 2000). In addition, CaN has been immunolocalized in the flame cells of the *Schistosoma* excretory system, and in the cilia of *Paramecium tetraurelia*, where it seems to be involved in the regulation of exocytosis (Mecozzi et al., 2000; Fraga et al., 2010).

CaN activity is regulated by its interaction with several endogenous proteins. Among CaN inhibitors are: AKAP79, which anchors CaN to the membrane with protein kinases A or C; cain/cabin 1, which binds to CaN, blocking its interaction with physiological substrates; the CaN-B homologous protein (CHP/p22), which mimics the interaction of the regulatory subunit CaN-B with CaN-A; and a family of regulators of CaN (RCAN), which bind directly to CaN-A (Rusnak and Mertz, 2000; Mellström et al., 2008). On the other hand, calpains, cytosolic Ca^{2+}-activated cysteine proteases, activate CaN in both a direct and an indirect manner by cleavage of CaN-A autoinhibitory domain and cain/cabin 1, respectively (Kim et al., 2002). In addition to the endogenous inhibitors, the immunosuppressant drugs cyclosporine A (CsA) and FK506 (tacrolimus), both produced by soil microorganisms, inhibit CaN signaling, allowing the elucidation of its function in many eukaryotic organisms. These drugs bind to cyclophilin (CyP) or FK506-binding protein (FKBP) and the CyP-CsA and FKBP-FK506 complexes inhibit CaN allosterically (Liu et al., 1991). Similarly, the intracellular chelator BAPTA (1,2-bis(o-aminophenoxy)ethane-N,N,N′,N′-tetracetic acid) which is highly selective for Ca^{2+} over Mg^{2+} has also been widely used as an inhibitor of the calcium–calcineurin pathway (Semsarian et al., 1999; Srinivasan et al., 2010).

Human cystic echinococcosis or hydatidosis is an endemic worldwide zoonosis caused by the larval or metacestode stage of the tapeworm *Echinococcus granulosus.* The complex life cycle of *E. granulosus* involves an intermediate host (humans and domestic livestock) and a definitive one (canid). The cyst or metacestode develops in the intermediate host and produces protoscoleces from the inner germinal layer. Protoscoleces develop into adult worms in the gut of the definitive host (McManus et al., 2003). However, *E. granulosus* shows another alternative development. Protoscoleces which are released into the circulation from a ruptured cyst, located in an intermediate host, are able to asexually differentiate into secondary hydatid cysts. This reveals an evident and high developmental plasticity.

The evaluation of the action of CsA on the establishment and growth of secondary hydatid cysts of *E. granulosus* in mice has indicated that this drug is a possible candidate for future clinical application (Hurd et al., 1993). Colebrook and collaborators (Colebrook et al., 2002, 2004) demonstrated that CsA is an effective protoscolicidal agent against *E. granulosus*, assessed the dose and time-dependent susceptibility from *in vitro* treated parasites and characterized one type of CyP involved in protoscolex drug sensitivity. In our laboratory, we have previously described the synergic protoscolicidal actions during the combined therapy with rapalogs and CsA and identified the two different cellular targets: FKBP-TOR and CyP-CaN (Cumino et al., 2010). We have also identified two genes homologous to the *Homo sapiens* CaN-A gene and one to the *Taenia asiatica* CaN-B gene in the *E. multilocularis* assembled genomic contigs, as well as their corresponding Expressed Sequence Tag (EST) in the *E. granulosus Lopho* DB (Cumino et al., 2010). In the present study, we focused on the biochemical and molecular characterization of CaN in the *E. granulosus* larval stages (Eg-CaN), its involvement in protoscolex exocytic processes and the identification of its possible endogenous regulators.

2. Materials and methods

2.1. In vitro *culture of protoscoleces, metacestodes and pre-microcyst obtainment*

E. granulosus protoscoleces were removed under aseptic conditions from hydatid cysts of infected cattle presented for routine slaughter at the abattoir in the province of Buenos Aires, Argentina. Protoscolex *in vitro* culture ($n = 3000/9.5\,cm^2$), pharmacological treatment and vitality assays were performed as previously described (Cumino et al., 2010). Otherwise, *E. granulosus* metacestodes (10–20 cysts for each drug treatment) were obtained from the peritoneal cavities of CF-1 mice after intraperitoneal infection with protoscoleces (Nicolao et al., 2014a). Animal procedures and management protocols were carried out as previously described (Nicolao et al., 2014b) in accordance with National Health Service and Food Quality (SENASA) guidelines, Argentina and with the 2011 revised form of The Guide for the Care and Use of Laboratory Animals published by the U.S. National Institutes of Health. Unnecessary animal suffering was avoided throughout the study. *In vitro* protoscolex and metacestodes treatments were assayed with CsA and BAPTA at 100 μM for 24 h. For molecular experiments, parasites were washed with sterile and RNAse-free PBS and they were conserved at −80 °C until experimental use. Each experiment was assayed for three replicates and repeated three times.

Incubation of protoscoleces with insulin and fetal bovine serum (FBS) for several days induces a progressive de-differentiation toward the metacestode stage or microcyst. Microcysts represent the phase in which the protoscolex is completely transformed into a miniature cyst (loosing suckers, rostellum and hooks, and showing a laminated layer), but the success rate of protoscoleces undergoing this de-differentiation process is very low (1–3%). However, a previous differentiation stage, named pre-microcysts can be obtained more easily. The pre-microcyst, a vesicle-like structure, is a completely vesicularized protoscolex with suckers and rostellum vestiges, without a laminated layer and almost devoid of movement (Cucher et al., 2013). In order to obtain vesicularized protoscoleces and pre-microcysts, aliquots of 1500 protoscoleces were cultured in Leighton tubes in medium 199 supplemented with antibiotics (penicillin, streptomycin and gentamicin 100 μg/ml), glucose ($4\,mg\,ml^{-1}$), insulin ($1.2\,U\,ml^{-1}$) and 15% FBS. A total of 30–40 tubes per sample were cultured and the protoscoleces from the same sample develop at different rates. Cultures were maintained at 37 °C for 50 days, the medium was changed every 4–6 days and the sample was carefully recovered after of the complete decantation. The pH was monitored during the culture period by means of the pH indicator (phenol red incorporated in the 199 medium) and adjusted with 5 mM HEPES (4-(2-hydroxyethyl)-1-piperazineethanesulfonic acid, pH 7.5) to control it within the normal physiological range. Development was followed microscopically under an inverted light microscope

every day. Meanwhile, the number of developed pre-microcysts was determined at different time points. Among 15–45 days, pre-microcysts developed under *in vitro* conditions were recovered and used for immunohistochemistry studies.

2.2. Gene identification, cloning and expression by reverse transcription (RT)-PCR and quantitative (q)-PCR

In order to obtain information on occurrence of *Echinococcus can*-A, *can*-B, *chp*, *cabin* and *calpain* sequences, the *E. multilocularis* genomic database, *E. granulosus* assembled genomic contigs (http://www.sanger.ac.uk/Projects/Echinococcus) and available sequences in the EST database of *E. granulosus* (http://www.nematodes.org/NeglectedGenomes/Lopho.php) were searched with BLASTp and tBLASTn programs. Sequences of *H. sapiens* and *S. mansoni* were used as queries. We identified a single sequence for each putative gene, including *can*-B, *chp* and *cabin*, but two homologs of *can*-A and five putative calpain genes. Specific primers were design and are listed in Supplementary Table S1.

Supplementary Table S1 related to this article can be found, in the online version, at http://dx.doi.org/10.1016/j.actatropica.2015.03.016.

Total RNA extractions, RT-PCR, cloning and qPCR were performed as previously described (Cumino et al., 2010). To analyze the levels of gene expression in control and CsA- and BAPTA-treated parasites, cDNA was generated from total RNA treated with DNAse (RQ1, Promega, USA), Superscript II reverse transcriptase (Invitrogen, Argentina) and Pfu (Promega, USA) DNA polymerase. Equal amounts of cDNA from protoscoleces and metacestodes were amplified in 30 cycle PCRs of 94 °C (30 seg), 45 °C (1 min), and 72 °C (1 min) plus a single step at 72 °C for 10 min. *E. granulosus* actin I (*act*-I, GenBank accession no. L07773) was used as a loading control. To determine the optimal amount of input RNA, the 3-fold diluted template RNA was amplified in RT-PCR and qPCR assays under identical reaction conditions to construct a standard curve for each gene product. Once the optimal amount of input RNA was determined for each gene product, RT-PCR and qPCR were carried out under identical reaction conditions to detect differential transcript levels of genes in the control and treated parasites. Under these conditions, PCR amplification occurs in the linear range. RT-PCR products were electrophoresed, purified using a Quiaquick PCR Purification Kit (Quiagen N° 28104, Argentina) and sequenced (Unidad Genómica, INTA Castelar, Argentina). In addition, qPCR experiments from parasites were carried out in a StepOne Applied Biosystems cycler for all studied genes. The second reaction mixture contained 0.5–1 μl cDNA, 12.5 μl of real mix (containing 0.1 μl of Taq DNA polymerase, Taq DNA polymerase buffer, 3 mM $MgCl_2$, 0.2 mM dNTPs and SYBR® GreenTM) and 50 pmol of each primer for each gene. The PCR program was at 95 °C (10 min), 40 cycles at 95 °C for 15 s, 50 °C for 30 s, and 72 °C for 30 s. Product identification was confirmed by a melting curve analysis and visualized on agarose gels. The relative rate of each cDNA was normalized using *act*-I (see above). Data analyses for a relative quantification of gene expression were performed by the comparative threshold cycle (Ct) method.

2.3. Sequence analysis

Orthologs were selected based on reciprocal best BLAST hits and with the presence of the characteristic domains in each deduced amino acid sequence. A list containing all of the identified *E. granulosus* genes was analyzed both manually and by BLASTp (after joining the conceptual translation of exons) against the GenBank nr (non-redundant) database. Sequence alignments were generated with the CLUSTALX software program. Modeling of tertiary structures was obtained from the deduced primary structure using the Gen-THREADER (SWISS-PROT).

2.4. Enzyme assays

Protein extracts were performed from pharmacologically treated and control protoscoleces and metacestodes according to Cumino et al. (2012). Protein phosphatase activity from crude extracts was measured using p-nitrophenyl phosphate (p-NPP) which is hydrolysed by phosphatases to p-nitrophenol (p-NP), a chromogenic product with absorbance at 405 nm. In all cases, the volume of the reaction mixture was 100 μl with a composition of 250 mM imidazole buffer (pH 7.2, for alkaline phosphatase inhibition), 0.5 mg ml^{-1} BSA, 0.1% β-mercaptoethanol, 10 mM $CaCl_2$, 20 mM p-NPP, 50 μl of protein extract (corresponding to 0.5 μg/μl) and selective tyrosine or serine–threonine (S/T) phosphatases inhibitors (Tonks et al., 1988; Hunter, 1995). Total S/T and tyrosine phosphatase activity were measured in presence of 50 μM vanadate (for tyrosine phosphatase inhibition) and 50 mM NaF, (for S/T phosphatase inhibition), respectively. PP2B activity was measured in presence of 1 mM EDTA (for chelating Mg^{+2} which is required for PP2C activity) and 50 nM okadaic acid (for PP2A inhibition). $NiCl_2$ (5 mM) was used as an activator of PP2B. PP2A and PP2C activities were determined in presence of 1 mM EGTA (for chelating Ca^{+2} which is required for PP2B activity) plus 1 mM EDTA or 50 nM okadaic acid, respectively. The reactions were conducted at 30 °C for 30 min and were terminated by the addition of 0.3 N NaOH. Changes in absorbance, measured at 405 nm, were used to calculate phosphatase activity. Three independent assays were carried out and each biochemical assay was done in duplicate.

2.5. Detection of exocytic processes in protoscoleces

Experiments to detect CaN-A involvement in exocytic processes were performed using FM4-64 (Invitrogen #T13320, Argentina, a lipophilic fluorescent dye) on control and CsA-treated protoscoleces. All experiments were carried out with 1×10^3 protoscoleces in a final volume of 100 μl of 50 mM HEPES buffer (pH 7.5) with 8 mg ml^{-1} glucose inside wells of a 96-well plate. Protoscoleces were incubated with 500 μM CsA or without drugs (control) for 3 h at 37 °C and then 25 μM FM4-64 were added to the solution for 45 min at 37 °C in the dark. After that, they were washed three times with dye free buffer in the dark and observed with an inverted confocal laser scanning microscope (Nikon, Confocal Microscope C1). In addition, fluorescence was recorded in a Fluoroskan II Acsent microwell fluorometer (Thermo Electron Company, Finland) every 10 s for 30 min (538 nm excitation–605 nm emission). Finally, the unloading kinetics of FM4-64 was determined after stimulation with 0.25 N HCl (were also assayed 20 μM glucose and 100 mM potassium chloride). Confocal images were collected every 30 s after discharge stimulation. Negative controls consist of protoscoleces incubated without FM4-64. All experiments were performed in duplicate and repeated three times.

2.6. Western blot analysis and evaluation of immunofluorescence by confocal microscopy

Polypeptides were separated by SDS-PAGE on 12% polyacrylamide gels and electroblotted onto a nitrocellulose membrane (Hy-Bond C; Amersham, Argentina) as previously described (Cumino et al., 2010). The membranes were incubated with a monoclonal antibody which recognizes an epitope located on the α-subunit of bovine calcineurin (anti-CaN α subunit, Sigma C1956 clone CA-A1, USA, 1:50 dilution) or with primary monoclonal antibody of human actin (JLA-20, Developmental Studies Hybridoma Bank-DSHB, USA, 1:2000 dilution) as a control for protein loading.

The anti-CaN-A antibody used in these assays is directed against an epitope which showed 69% amino acid identity with the possible orthologs of *E. granulosus*. Additionally, *in toto* immunohistochemistry was carried out as previously described (Nicolao et al., 2014a). Control and pharmacologically treated protoscoleces or pre-microcyst were incubated for 4 days at 4 °C with primary anti-CaN-A antibody or with primary polyclonal antibody of human ATP-dependent DDX6 RNA helicase (Bethyl A300-461 A, USA, 1:100 dilution), and washed with PBS for 24 h at 4 °C. Then, they were incubated with goat anti-mouse IgG conjugated with FITC for 2 h at room temperature or goat anti-rabbit IgG conjugated with Cy3 for 24 h at 4 °C, respectively. Antibody penetration into developing cyst was checked using anti-DDX6 as positive control. Finally, parasites were washed and counterstained with 2 μg/ml propidium iodide (Molecular Probes P-3566, Argentina, to observe all cell nuclei under optimal contrast conditions, except in presence of anti-DDX6 because it is conjugated with Cy3). They were observed with an inverted confocal laser scanning microscope (Nikon, Confocal Microscope C1). Negative controls consisted of omission of primary antibody for both experiments. The intensities of green (excitation/emission wavelength = 485/538 nm) fluorescence were analyzed for 20× images from control and treated-protoscoleces and for 5× images from individual pre-microcysts in control conditions. Regions of interest including protoscoleces, vesicularized protoscoleces and pre-microcyst were selected and the mean fluorescence intensity per area was calculated. Excitation and detection of the samples were carried out in sequential mode to avoid overlapping of signals. Sections were scanned with laser intensity, confocal aperture, gain and blacklevel setting kept constant for all samples. Optical sections were obtained at increments of 0.3 mm in the *z*-axis and were digitized with a scanning mode format. Background fluorescence was subtracted and immunofluorescence intensity (IF) was calculated as the average for each selected area. The fluorescence intensity at the selected areas, linearly correlated with the number of pixels, was quantitatively analyzed using standard imaging analysis from Image J software (NIH, http://rsb.info.nih.gov/ij/).

2.7. Statistics

Data within experiments were compared and significance was determined using the student's *t* test and $p < 0.05$ was considered statistically significant. All data are shown as arithmetic mean ± SEM.

3. Results

3.1. Occurrence and expression of calcineurin genes from E. granulosus larval stages

Extensive tBLASTn searches on the available *E. multilocularis* genome and the incompletely assembled *E. granulosus* genome revealed the presence of two *can*-A genes and one *can*-B gene coding for the CaN-A1, CaN-A2 and CaN-B putative proteins, respectively. The coding regions for Eg-*can*-A1 and Eg-*can*-B were cloned, fully sequenced and annotated in GenBank (KC146906.1 and HQ454284.2, respectively) before genome publication. Then, the predicted genes for Eg-*can*-A1, Eg-*can*-A2 and Eg-*can*-B were respectively annotated as EgrG_000601200 (EgG_scaffold_0003, positions 2834653–2858254), EgrG_001157700 (EgG_scaffold_0029, positions 183630–233465) and EgrG_000454300 (EgG_scaffold_0004, positions 3078453–3079199) in the GeneDB database. RT-PCR analysis indicated expression of the Eg-*can*-A1 and Eg-*can*-B genes in protoscoleces and metacestodes (Fig. 1A). To investigate whether cytosolic-free Ca^{2+} concentration levels affect the expression of the regulatory subunit gene, protoscoleces and metacestodes were treated with BAPTA for 24 h, and transcriptional levels were estimated by qPCR. BAPTA decreased the level of Eg-*can*-B mRNA respect to controls in both larval stages (Fig. 1B). On the other

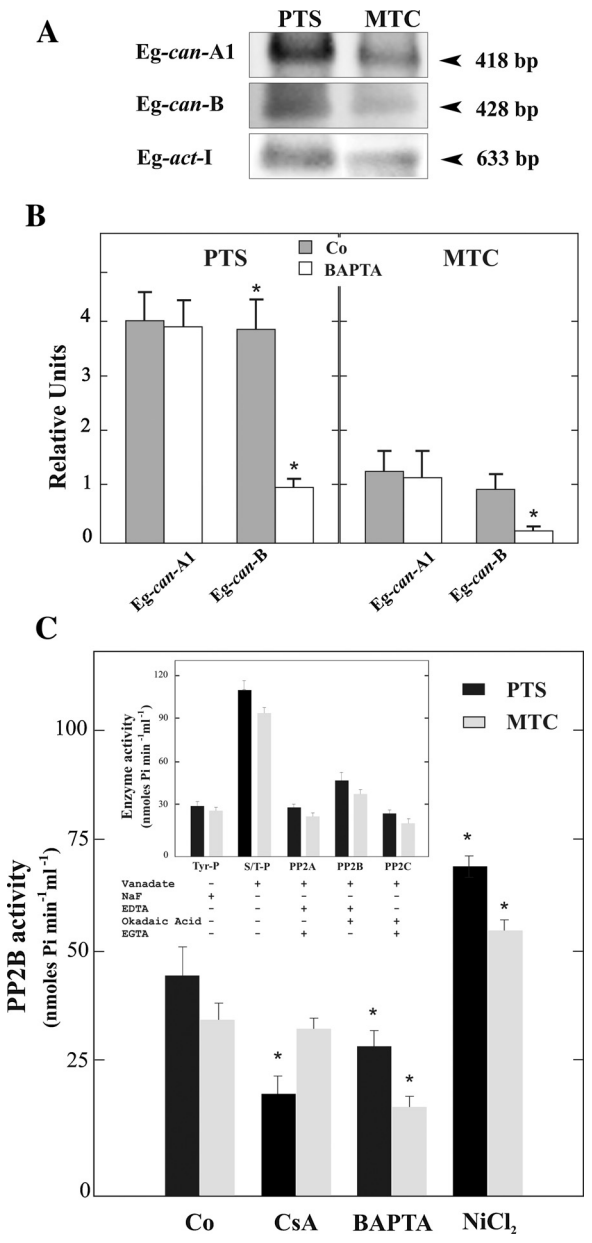

Fig. 1. Calcineurin expression in *E. granulosus* larval stages. (A) Reverse transcription (RT)-PCR analysis of Eg-*can*-A1 and Eg-*can*-B genes from total RNA of control protoscoleces (PTS) and metacestodes (MTC). Amplification of Eg-*actin*-I (Eg-*act*-I) was used as an internal control. Molecular sizes of amplicons are indicated with arrowheads. (B) Quantitative PCR (qPCR) from RNA of PTS and MTC incubated for 24 h under control conditions (Co) or treated with 100 μM BAPTA. Amplification of Eg-*actin*-I (Eg-*act*-I) was used as an internal control. Values are mean ± S.D. of three independent experiments. Asterisks indicate significant differences. (C) Determination and modulation of 2B protein phosphatase (PP2B) activity in *E. granulosus* larval stages. Total protein phosphatase activities from crude protein extracts of protoscoleces (PTS) and metacestodes (MTC) were measured using p-nitrophenyl phosphate (p-NPP) in presence of imidazole buffer and selective tyrosine or serine–threonine phosphatases inhibitors. Tyrosine (Tyr) and total serine/threonine phosphatase (S/T-P) activities are shown in the inset. Modulators of PP2B activity were 100 μM CsA, 100 μM BAPTA and 10 μM $NiCl_2$. The values represent mean ± S.D. ($n = 3$). Asterisks indicate significant differences.

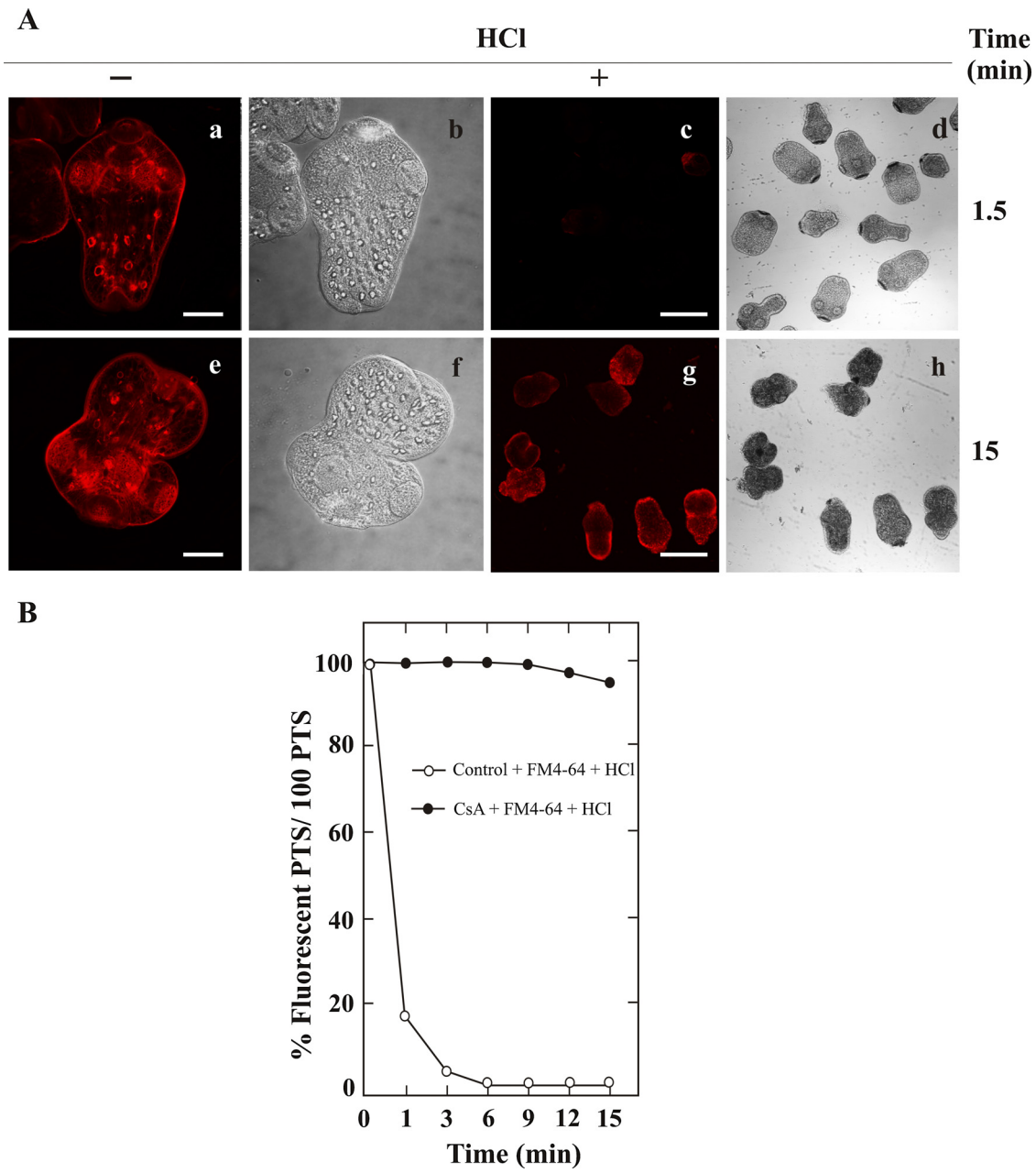

Fig. 2. Involvement of *E. granulosus* calcineurin in exocytic processes of protoscoleces. (A) Confocal images of control (a and c) and CsA-treated protoscoleces (e and g) incubated with FM4-64 and their corresponding photomicroscopy of light field (control, b and d; CsA-treated f and h). FM4-64 was loaded in both sample types and dye-staining was observed in the inner membrane systems, tegument and excretory bladder (a and e). The unloading kinetics of FM4-64 was determined after stimulation with HCl (+) and recorded after 1.5 min and 15 min of HCl exposure. (B). FM4-64 unloading kinetics determined after stimulation with 0.25 N HCl. CsA-treated protoscoleces retained staining even 15 min after stimulus.

hand, the transcriptional level of Eg-*can*-A was similar in control and BAPTA-treated parasites (Fig. 1B).

The predicted Eg-CaN-A1 sequence aligned with 74, 73 and 98% identity with the *H. sapiens* (AAG02563), *S. mansoni* (CAB93676) and *E. multilocularis* (EmuJ_000601200) orthologs, respectively, and contains all conserved domains required for substrate dephosphorylation, including the catalytic subunit and the regulatory subunit with the CaN-B binding domain, the CaM-binding domain and the autoinhibitory site (Supplementary Fig. S1A and B). Sequence analysis revealed that two Eg-CaN-A1 and Eg-CaN-A2 isoforms with 68% identity display a high degree of sequence conservation in the catalytic (with the invariant phosphoprotein phosphatase-PPP-motif-GDXHG- and conserved SAPNYL motif) and regulatory domains (region between 15 and 500 residues) varying in their N- and C-terminal regions (Supplementary Fig. S1B and data not shown). On the other hand, Eg-CaN-B, a small protein of 169 amino acids, aligned with 87, 92 and 100% identity with the *H. sapiens* (AAB08721), *S. mansoni* (CAB93677) and *E. multilocularis* (EmuJ_000454300) orthologs, respectively. This protein conserves four EF-hand domains which are essential for Ca^{2+}-dependent phosphatase activity and preserve the characteristic glycine residues, which represent conserved myristoylation sites (Supplementary Fig. S1A–C).

Supplementary Fig. S1 related to this article can be found, in the online version, at http://dx.doi.org/10.1016/j.actatropica.2015.03.016.

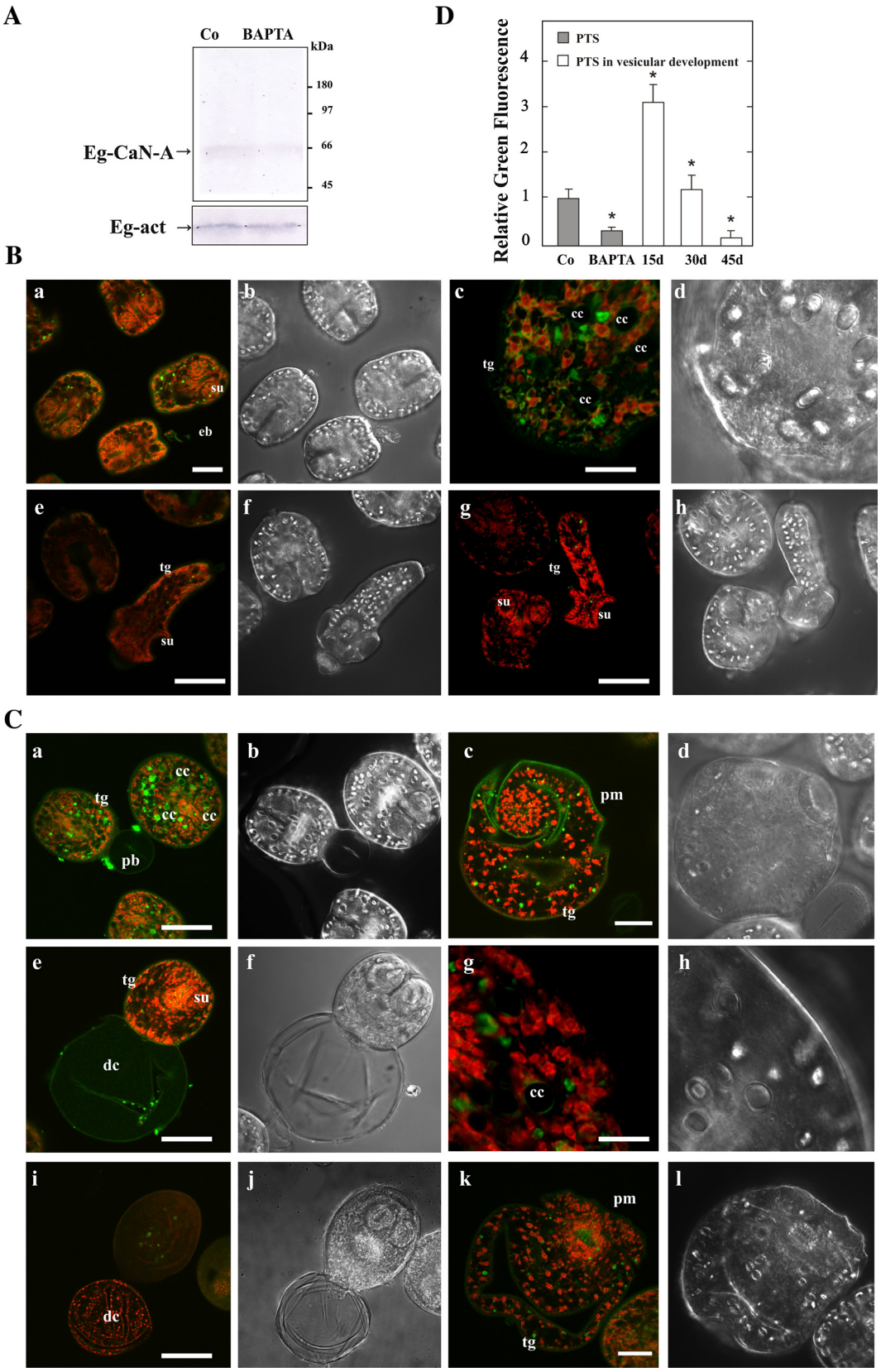

Fig. 3. Detection and *in situ* localization of Eg-CaN-A from *Echinococcus granulosus* protoscoleces and *in vitro*-develop cyst. (A) Immunoblot of Eg-CaN-A revealed with a heterologous antibody against bovine CaN-A. Total protein extracts from control (Co) and 100 μM BAPTA-treated protoscoleces (BAPTA) were loaded at 100 μg of total protein/lane. Anti-human-actin was used as loading control. Polypeptide sizes are shown. (B) *In situ* immunolocalization of Eg-CaN-A in *E. granulosus* protoscoleces. Confocal images of *in toto* immunofluorescence assays performed with the same antibody anti-CaN-A conjugated with FITC – green fluorescence and counterstained with propidium iodide – red fluorescence. Eg-CaN-A expression in control (a–d), and in BAPTA-treated protoscoleces (e–h). Confocal (a, c, e and g); transmission images (b, d, f and h); eb, excretory bladder; su, sucker; tg, tegument; cc, calcareous corpuscle. (C) Immunolocalization of Eg-CaN-A during the vesicular development to pre-microcyst. Confocal images were obtained with the same antibody anti-CaN-A conjugated with FITC – green fluorescence and counterstained with propidium iodide (red fluorescence, a–j) or

3.2. Protein phosphatase assay in E. granulosus larval stages

To investigate the PP2B activity of Eg-CaN, protein extracts from control or pharmacologically treated protoscoleces and metacestodes were incubated in the presence of selective tyrosine and S/T protein phosphatase inhibitors. Total S/T protein phosphatase activity was determined in both larval stages and PP2B activity accounted for 40% (45 ± 5 nmol Pi min^{-1} ml^{-1} in protoscoleces and 32 ± 4 nmol Pi min^{-1} ml^{-1} in metacestodes) of the total activity (110 ± 10 nmol Pi min^{-1} ml^{-1} in protoscoleces and 92 ± 10 nmol Pi min^{-1} ml^{-1} in metacestodes), indicating that, in *E. granulosus*, Eg-CaN corresponds to an active protein phosphatase (inset Fig. 1C). Treatment with 100 μM CsA caused 60% inhibition of protoscolex PP2B activity, while in metacestodes the enzymatic activity was similar to that of the controls (Fig. 1C). In addition, treatment with 100 μM BAPTA negatively regulated PP2B activity in both larval stages (PP2B activity was inhibited 40–50% respect to the control), suggesting a calcium regulation of CaN phosphatase activity (Fig. 1C). We also observed higher PP2B activity in the presence of Ni^{+2} respect to the basal activity observed in controls (the specific phosphatase activity was enhanced to 50–70% of the control), indicating that this metal ion is an effective activating cofactor in both larval stages (Fig. 1C).

3.3. Involvement of CaN in exocytic processes in protoscoleces

To determine whether Eg-CaN was involved in exocytic processes, we performed an assay using FM4-64. FM4-64 was first loaded in control and CsA-treated protoscoleces and dye-staining was observed in the inner membrane systems, tegument and excretory bladder (Fig. 2A(a and e)). The unloading kinetics of FM4-64 was standardized with different exocytic inducers using a fluorskan to record the fluorescence (data not shown). Then, the samples were exposed to an unloading stimulation with 0.25 N HCl to evaluate the exocytic kinetics of FM4-64. Sequential images were captured every 30 s during the releasing process (Fig. 2A). In control protoscoleces, FM4-64 was completely discharged 1.5 min after the stimulus, whereas in CsA-treated larvae, staining was observed even 15 min after the stimulus (Fig. 2A(c and g) and B). This suggests that, in *E. granulosus* protoscoleces, CaN is specifically involved in exocytic activity.

3.4. Expression pattern of Eg-CaN-A during larval stage and microcyst development

Using a heterologous monoclonal antibody directed against the α-subunit of bovine CaN, which showed 79 and 73% amino acid identity with Eg-CaN-A1 and Eg-CaN-A2, respectively, both proteins may be detected by immunoassays. A single band of the expected size at 66 kDa was more intense in control than in BAPTA-treated protoscoleces (Fig. 3A).

In toto immunofluorescence labeling showed that anti-CaN-A reactivity was localized in the cytoplasm of tegumental cells, suckers and excretory bladder of protoscoleces (Fig. 3B(a–d)). Protoscoleces treated with 100 μM BAPTA showed a three-fold decrease in the fluorescence intensity compared to the control, which indicates a reduction in Eg-CaN-A expression in the presence of Ca^{2+} chelators (Fig. 3A, B(e–h) and D). Moreover, at the beginning of vesicular differentiation (15 days, Fig. 3C(a–d)), the fluorescence intensity of Eg-CaN-A was 3.5-fold higher than in control protoscoleces (Fig. 3D). This was mainly observed in the posterior bladder and in the complete cellular territory (especially around the calcareous corpuscles) of vesicularized protoscoleces (Fig. 3C(a–d)) according to the morphological description made by Rogan and Richards (1986). At 30 days of this process (Fig. 3C(e–h)), Eg-CaN-A fluorescence intensity was two-fold lower than at 15 days of development and at 45 days Eg-CaN-A was almost undetectable (Fig. 3C(i–l) and D). However, simultaneously, we detected high DDX-like RNA helicase expression (red fluorescence – Fig. 3C(k–l)) in the new developing cyst. The protein coding gene is annotated as EgrG_000123700 in GeneDB database and its gene product showed 89% identity with the human ortholog. No immunoreactivity was detected in samples lacking the primary antibody.

3.5. Occurrence and gene expression of calcineurin endogenous regulators in E. granulosus larval stages

To evaluate the occurrence and gene expression of CaN endogenous regulators, extensive tBLASTn searches were carried out in the incompletely assembled *E. granulosus* genome. Ortholog selection was based on reciprocal best hits in BLAST searches, using an E-value cutoff $\leq 1e^{-25}$. We identified a single sequence for *chp* and its coding region was cloned, fully sequenced and annotated in GenBank (KC146907.1). On the other hand, *cabin* and five putative *calpain* (*calp*) genes were also identified and annotated as EgrG_001065650, EgrG_000911200, EgrG_000319100, EgrG_000719700, EgrG_000253150 and EgrG_000205500 in the GeneDB database, respectively.

RT-PCR analysis indicated expression of all the CaN-regulator genes identified in protoscoleces and metacestodes (Fig. 4A). In protoscoleces, qPCR showed lower mRNA expression levels for Eg-*chp* (three-fold), Eg-*cabin* (one-fold), Eg-*calp*-A (one-fold), Eg-*calp*-B (one-fold) and Eg-*calp*-E (two-fold) in 100 μM BAPTA-treated protoscoleces than in controls (Fig. 4B). On the other hand, the transcript levels for Eg-*calp*-C and Eg-*calp*-D from BAPTA-treated protoscoleces and all the genes studied in metacestodes were similar to those of the controls (Fig. 4B and C).

The predicted proteins for all CaN-endogenous regulators analyzed in this work presented a high degree of conservation with eukaryotic orthologs. Eg-CHP presented a high degree of similarity with Eg-CaN-B (38% identity) and Eg-CaMs (24–36% identity) and showed 52% identity with *H. sapiens* CHP. The predicted polypeptide sequences of Eg-Cabin and Eg-Calp-A-E aligned with 28, 40, 35, 34, 31 and 25% identity with *H. sapiens* orthologs, respectively (Supplementary Fig. S2). These proteins showed that all domains corresponding to specific functions were conserved. Eg-Calp-A and Eg-Calp-B correspond to classical calpains since they possess the C2-like and the EF-hand domains, whereas Eg-Calp-C, Eg-Calp-D and Eg-Calp-E exclude the C2-like and/or the EF-hand domains according to the non-classical calpains (Supplementary Fig. S2). The finding that the Eg-*can*-B gene and the regulatory protein encoding genes were down-expressed in BAPTA-treated protoscoleces led us to investigate the possible presence of Ca^{2+}-sensitive transcription factors in the *E. granulosus* genome. We identified the following Ca^{2+}-dependent transcriptional factors: a single NF-Y-like complex (three subunits, α, β and γ, are EgrG_000204400, EgrG_00106-1700, EgrG_000459200 or EgrG_000459300, respectively), two AP- (EgrG_000768400 and EgrG_000457200) and five ETS-like proteins (EgrG_000995300, EgrG_001099200, EgrG_000751100, EgrG_000770200 and EgrG_000770300), as described in other

co-incubated with anti-DDX6 conjugated with Cy3 (red fluorescence, k–l) used as antibody penetration control. Protein expression changes were recorded at 15 (a–d), 30 (e–h) and 45 days (i–l) of vesicular differentiation. Confocal (a, c, e, g, i, k) and transmission images (b, d, f, h, j, l); pb, posterior bladder; cc, calcareous corpuscles; tg, tegument; su, sucker; dc, developing cyst; pm, pre-microcyst. (D) Normalized fluorescence values of Eg-CaN-A expression in protoscoleces (gray bars: control – Co and BAPTA-treated – BAPTA) and parasites in vesicular development (open bars: at 15, 30 and 45 days – 15d, 30d, 45d, respectively – of development in presence of insulin and SFB). Data represents three independent experiments with twenty or five parasites per experiment ($n = 60$ and $n = 15$). Scatter bars correspond to SEM.

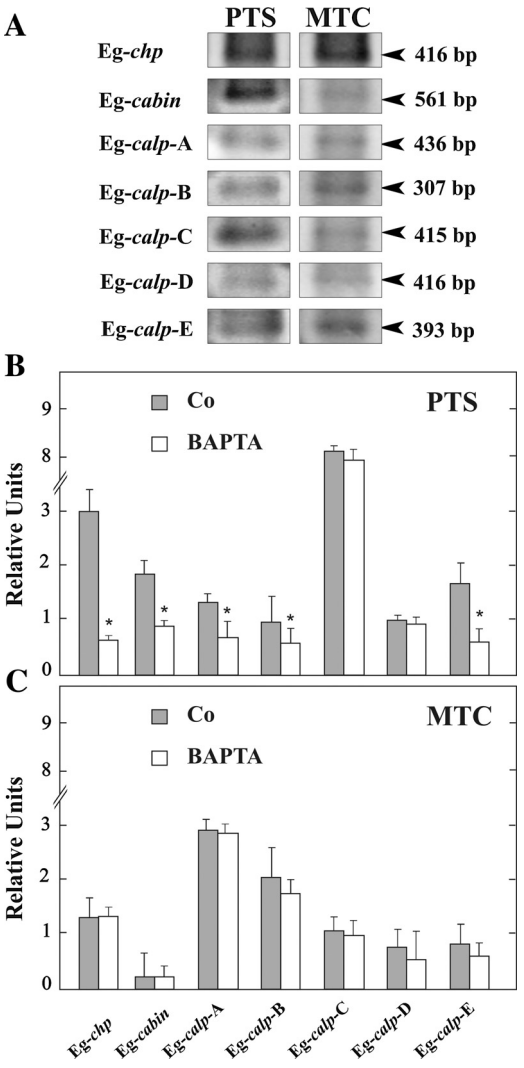

Fig. 4. Gene expression of calcineurin endogenous regulators in *E. granulosus* larval stages. (A) RT-PCR analysis of Eg-*chp*, Eg-*cabin* and Eg-*calp*-(A–E) genes from total RNA of control protoscoleces (PTS) and metacestodes (MTC). Molecular sizes of amplicons are indicated with arrowheads. (B) Quantitative PCR (qPCR) analysis of Eg-*chp*, Eg-*cabin* and Eg-*calp*-(A–E) genes from total RNA of protoscoleces (PTS) incubated for 24 h under control conditions (Co) or treated with 100 μM BAPTA. (C) qPCR assay of these genes from total RNA of metacestodes (MTC) carried out under the same conditions as indicated in (B). Values are mean ± S.D. of three independent experiments. Asterisks indicate significant differences.

metazoa. Alignment of the amino acid sequence of these putative transcription factors with orthologous factors revealed that the DNA binding domain is highly conserved (data not shown).

Supplementary Fig. S2 related to this article can be found, in the online version, at http://dx.doi.org/10.1016/j.actatropica.2015.03.016.

4. Discussion

The regulation of cell function by protein phosphorylation is controlled by an equilibrium between protein kinases and phosphatases. In contrast to the many Ca^{2+}-dependent protein kinases, CaN is the only known protein phosphatase under the control of this cation and CaM. Thus, it may play a critical role in the coupling of calcium signal to physiological responses in all ion-sensitive cells. In this work, we demonstrated *Echinococcus* CaN activity and its calcium regulation. Furthermore, we characterized CaN molecularly and immunolocalized Eg-CaN-A.

Based on sequence information obtained from the *Echinococcus* genome project, we identified two genes coding for the catalytic Eg-CaN-A subunit and one gene coding for the regulatory Eg-CaN-B subunit that were constitutively expressed in larval stages (Fig. 1A, Supplementary Fig. S1, Tsai et al., 2013; Zheng et al., 2013). This is similar to what has been observed in other eukaryotic organisms (Rusnak and Mertz, 2000). The Eg-*can*-A1 and Eg-*can*-B genes were upregulated in protoscoleces respect to metacestodes in accordance to that found by Zheng et al. (2013). Their predicted proteins showed considerable evolutionary conservation of the sites interacting with each other, as compared with their mammalian counterparts. The C-terminal portion of all CaN-A, including Eg-CaN-A isoforms, contains a regulatory domain with a highly hydrophobic CaN-B binding site, with the critical residues for interaction with CyPs and FKBPs, followed by the CaM-binding domain and the autoinhibitory domain (Supplementary Fig. S1A and B, Klee et al., 1998). The configuration of the catalytic domain in Eg-CaN-A1 and Eg-CaN-A2 presents the characteristic invariant PPP motifs and the highly conserved SAPNYL sequence, as described in human and helminth orthologs (Klee et al., 1998; Connor et al., 1999). These holoenzymes are associated with Fe^{2+} and Zn^{2+}, both activating cofactors for their active sites (King and Huang, 1984). On the other hand, as it has already been described in other orthologs, Eg-CaN phosphatase is *in vitro* activated by Ni^{2+} and Ca^{2+} (Fig. 1C, Klee et al., 1998; Rusnak and Mertz, 2000; Orrego et al., 2014). Nickel is vital to the structural and catalytic properties of the enzyme, indicating that it tightly binds the protein and it might have a role in the regulation of the substrate specificity of CaN (King and Huang, 1984). In the human genome, CaN-A exists in three distinct isoforms (α, β, and γ), which possess different substrate specificities and contribute to a precise regulation of CaN functions in different tissues (Kilka et al., 2009). In *E. granulosus*, sequence analysis showed that the catalytic and regulatory domains of the two Eg-CaN-A isoforms are highly conserved and that their N-terminal regions lack a consecutive poly-proline motif which is characteristic of the CaN-A β isoforms (Perrino et al., 2002). Thus, the N- and C-terminus of Eg-CaN-A isoforms display a high degree of sequence identity with the α and γ isoforms.

Since Eg-CaN-A isoforms retain the residues from the CsA-CyP and FK506-FKBP interaction (Supplementary Fig. S1, Cumino et al., 2010), both complexes should bind to the interaction region of Eg-CaN-A and Eg-CaN-B. This could thus prevent the conformational change of Eg-CaN-A required for its activation in a similar way as in its mammalian counterpart (Lin et al., 1999). Seven CyPs have been identified in the *Echinococcus* genome (Zheng et al., 2013). These CyPs seem to be of considerable importance to the mechanism of action of CsA (Colebrook et al., 2002; Cumino et al., 2010). Interestingly, the apparently constitutive active form of cystic-CaN (CsA insensitive activity, Fig. 1C) may indicate that calcium signaling *via* CaN appears to be different in protoscoleces when compared to cyst. This could be due to the presence of CyP isoforms resistant to CsA (Rusnak and Mertz, 2000) and/or highly expressed calpain isoforms that may convert the cystic Eg-CaN-A subunit into a constitutively active form (Fig. 4C and Shioda et al., 2006). Further studies in metacestodes are required to determine the characterization and expression of CyP isoforms and the physiological relevance of active CaN under basal conditions.

Echinococcus CaN-B also represents an evolutionarily conserved protein which shows four EF-hand Ca^{2+} loops with conserved glycine residues, which represent myristoylation sites in all eukaryotes (Supplementary Fig. S1C, Rusnak and Mertz, 2000). In protoscoleces and metacestodes, the intracellular concentration of Ca^{2+} transcriptionally regulates the Eg-*can*-B gene (Fig. 1B). This study provided the first evidence for a role of calcium in *Echinococcus* gene expression. Similarly, Eg-CHP, which is another EF-hand protein, conserves the Eg-CaN-A interacting sites. This

protein prevents allosteric activation of Eg-CaN-A (Lin et al., 1999) and it is transcriptionally regulated by Ca^{2+} only in protoscoleces (Fig. 4B). In this line of evidence, we identified Ca^{2+}-sensitive transcription factors such as NF-Y, AP and ETS-like proteins in the *Echinococcus* genome (data not shown). Transcriptional regulation of CaN-encoding genes has been corroborated in cardiac myocytes and neurons, demonstrating that the enhancer promoter region (between −3 to −1 kb) contains regulatory sequences that are important for Ca^{2+} inducibility (Oka et al., 2005; Cha-Molstad et al., 2012). Additionally, the Eg-CaN activity and protein level of Eg-CaN-A were highly decreased during the chelation of intracellular Ca^{2+} in BAPTA treatment (Figs. 1C and 3B (e-h)). In agreement with the present results, previous studies have demonstrated that CaN activity is strictly dependent on Ca^{2+} levels. Furthermore a sustained – not transient oscillatory – increases in Ca^{2+} level is necessary for CaN activation (Semsarian et al., 1999; Oka et al., 2005; Srinivasan et al., 2010; Cumino et al., 2010).

The regulated secretion is a Ca^{2+}- and CaN-dependent fundamental process underlying the function of many cell types (Pang and Südhof, 2010; Bennett et al., 2010). Stimulatory and inhibitory roles for CaN in regulated exocytosis have also been reported (Raufman et al., 1997; Høy et al., 2001). Our results suggest that at least one Eg-CaN-A isoform is involved in facilitating exocytosis, because this process was inhibited in CsA-treated protoscoleces (Fig. 2). In most cell types, certain Ca^{2+}-binding proteins participating in exocytosis, such as the dynamin, dephosphins, actin and kinesin, have been identified as substrates of CaN. Particularly, synaptotagmins are CaN targets in the secretion process, independently of NFATc intervention (Bennett et al., 2010). These proteins are expressed in all metazoa as Ca^{2+} sensors for exocytosis (Chapman, 2008) and 10 predicted orthologs have been identified in the *Echinococcus* genome (Tsai et al., 2013). Exocytosis represents a well-known tegumental and cellular process in this cestode, in which synaptotagmins could be involved in key membrane trafficking pathways in a CaN-dependent manner. In addition, CHP might act as a Ca^{2+} sensor for constitutive exocytosis, because it undergoes conformational change upon Ca^{2+} binding, is widely expressed and is required for vesicle targeting/fusion. Nevertheless, the molecular mechanisms of action of CHP in constitutive exocytosis remain unknown (Di Sole et al., 2012).

It is remarkable that NFATc orthologs are absent both in the *Echinococcus* genome and in nematodes (Graef et al., 2001). Thus, the absence of NFATc genes in invertebrates constitutes an important evolutionary aspect of CaN signaling (Schulz and Yutzey, 2004). However, one NFAT5-like ortholog (ID gene EmuJ_000600800 and EgrG_000600800) was identified in the *Echinococcus* genome. NFAT5 (also named Tonicity responsive Enhancer-Binding Protein – TonEBP), a primordial member of the Rel/NF-κB family, is an important component of the hyperosmolar stress response system in vertebrates and invertebrates (Drews-Elger et al., 2009). NFAT5 lacks the CaN-interaction motifs that are characteristic of NFATc proteins, but is induced by a different CaN-dependent mechanism (Trama et al., 2000; Li et al., 2007). Future studies must be carried out on the possible role of *Echinococcus* NFAT5 in relationship with Eg-CaN signaling. In addition, a MEF-2 ortholog (EmuJ_001027200) was identified in the *Echinococcus* genome. It is plausible that, as in vertebrates, MEF2 proteins may serve as tissue-specific end points of CaN signaling in both worms and flies (Gajewski et al., 2003).

In the same way as the protozoan CaN-A, Eg-CaN-A was identified as a cytoplasmic protein (Fig. 3B(a–d), Orrego et al., 2014). It is noteworthy that striking differences in Eg-CaN-A expression were observed during the asexual microcyst development from protoscoleces (Fig. 3C). Eg-CaN-A expression level first increased (15 days) but then progressively decreased during the development of the microcyst until it was undetectable (45 days, Fig. 3D). Moreover, simultaneous confocal detection of Eg-DDX-like RNA helicase allowed confirming the antibody penetration in the developing cyst while Eg-CaN expression was undetectable. Therefore, Eg-CaN expression changes during this developmental process toward the metacestode stage. In this line of evidence, recent reports have shown an inverse relationship between CaN activity and growth rate, which strongly supports that CaN is involved in the regulation of coordinated growth, acting as a molecular switch and involving intermittent CaN activity (Kujawski et al., 2014).

The occurrence and expression of Eg-cain/cabin and at least five Eg-calpain isoforms have been reported in different *E. granulosus* stages, being upregulated in protoscoleces, adults and cysts respect to oncospheres (Zheng et al., 2013). In agreement with these previous reports, our results showed that C and D calpain isoforms are overexpressed in protoscoleces respect to metacestodes, and that A and E calpain expression is higher in metacestodes. Besides, the down-expression of these genes in the presence of Ca^{2+} chelators (except Eg-*calp*-C and Eg-*calp*-D) suggests a complex regulation of CaN only in *Echinococcus* protoscoleces (Fig. 4B). In metacestodes, the expression of CaN regulators does not respond to Ca^{2+} availability (Fig. 4C), suggesting that cyst Eg-CaN could be controlled by other cell signals besides calcium concentration (Fig. 1B). Cain/cabin is a CaN inhibitor, but under certain conditions, it is cleaved by Ca^{2+}-activated calpain, leading to CaN activation (Kim et al., 2002). Thus, CaN activation and cain/cabin1 inactivation are calpain-dependent proteolysis (Kim et al., 2002), showing that these Ca^{2+}-dependent neutral proteases increase CaN phosphatase activity. It has been demonstrated that calpain-induced proteolysis of CaN occurs only at a conserved leucine site (L^{424}) of CaN-A, including Eg-CaN-A isoforms (Supplementary Fig. S1). Since total CaN activity depends on the participation of regulating and scaffold proteins, only *in vivo* experimental designs could allow finding out the final activity of CaN in this cellular system.

In this work we demonstrated the Eg-CaN expression in relationship with the exocytic processes and during the cyst development in *E. granulosus*, both key physiological events of the parasite life cycle. Many authors suggest CaN as a potential chemotherapeutic target against pathogenic organism (Chen et al., 2010; Orrego et al., 2014; Singh et al., 2014). However, in view of the fact that CaN is expressed in most tissues in the body and its inhibition with CsA or FK506 alters many cellular processes besides immune cell activation, the therapeutic use of CaN inhibitors is limited by serious side effects. Nevertheless, drugs that specifically and directly target calcineurin (Rodríguez et al., 2009) but lack the immunosuppressant activity, or calpain inhibitors (Wu et al., 2007) that block calpain-dependent CaN activation may have promise as antiechinococcal agents. Future studies should lead to the differential structure characterization of these parasite proteins, and assess them as new therapeutic targets against helminth diseases.

Acknowledgments

The authors gratefully acknowledge Prof. Dr. Graciela L. Boccaccio (Fundación Instituto Leloir, CONICET Universidad de Buenos Aires, Argentina) for the teaching guidance during Inter-U fellowship and for the DDX6 antibody provision and Lic. Daniela Villamonte (CONICET, Universidad Nacional de Mar del Plata) for the technical assistance with confocal microscopy. We also thank the use of facilities at the IIB-CONICET-UNMdP and at the INBIOTEC-CONICET-FIBA, Argentina and especially Dr. Salerno G. L. and Dr. Nöel Martinez G. A. Fluorescent dye FM4-64 was kindly provided by Prof. Dr. Laura de la Canal (Universidad Nacional de Mar del Plata CONICET, Argentina) and α-subunit CaN antibody by Prof. Dr. Luis Mayorga, (Universidad Nacional de Cuyo, CONICET, Argentina). This work was supported by Universidad Nacional de Mar del Plata (Grant EXA 572/12) and ANPCyT (PICT 2012, N°2668) Argentina. The *E. multilocularis* and *E. granulosus* genome sequences

data mentioned was produced by the Pathogen Sequencing Group of the Wellcome Trust Sanger Institute (Program of Helminth Sequencing; project manager: Dr. Matt Berriman).

References

Aramburu, J., Heitman, J., Crabtree, G.R., 2004. Calcineurin: a central controller of signalling in eukaryotes. EMBO Rep. 5, 343–348.

Bandyopadhyay, J., Lee, J., Bandyopadhyay, A., 2004. Regulation of calcineurin, a calcium/calmodulin-dependent protein phosphatase, in *C. elegans*. Mol. Cells 18, 10–16.

Banerjee, C., Sakar, D., Bhaduri, A., 1999. Ca^{2+} and calmodulin-dependent protein phosphatase from *Leishmania donovani*. Parasitology 118, 567–573.

Bennett, J.C., Roggero, C.M., Mancifesta, F.E., Mayorga, L.S., 2010. Calcineurin-mediated dephosphorylation of synaptotagmin VI is necessary for acrosomal exocytosis. J. Biol. Chem. 285, 26269–26278.

Cha-Molstad, H., Xu, G., Chen, J., Jing, G., Young, M.E., Chatham, J.C., Shalev, A., 2012. Calcium channel blockers act through nuclear factor Y to control transcription of key cardiac genes. Mol. Pharmacol. 82, 541–549.

Chapman, E.R., 2008. How does synaptotagmin trigger neurotransmitter release? Annu. Rev. Biochem. 77, 615–641.

Chen, Y.L., Kozubowski, L., Cardenas, M.E., Heitman, J., 2010. On the roles of calcineurin in fungal growth and pathogenesis. Curr. Fungal Infect. Rep. 4, 244–255.

Colebrook, A.L., Jenkins, D.D., Lightowlers, M.W., 2002. Anti-parasitic effect of cyclosporin A on *Echinococcus granulosus* and characterization of the associated cyclophilin protein. Parasitology 125, 485–493.

Colebrook, A.L., Jenkins, D.J., Jones, M.K., Tatarczuch, L., Lightowlers, M.W., 2004. Effect of cyclosporin A on the survival and ultrastructure of *Echinococcus granulosus* protoscoleces *in vitro*. Parasitology 129, 497–504.

Connor, J.H., Kleeman, T., Barik, S., Honkanen, R.E., Shenolikar, S., 1999. Importance of the b12–b13 loop in protein phosphatase-1 catalytic subunit for inhibition by toxins and mammalian protein inhibitors. J. Biol. Chem. 274, 22366–22372.

Cucher, M., Mourglia-Ettlin, G., Prada, L., Costa, H., Kamenetzky, L., Poncini, C., Dematteis, S., Rosenzvit, M.C., 2013. *Echinococcus granulosus* pig strain (G7 genotype) protoscoleces did not develop secondary hydatid cysts in mice. Vet. Parasitol. 193, 185–192.

Cumino, A.C., Lamenza, P., Denegri, G.M., 2010. Identification of functional FKB protein in *Echinococcus granulosus*: its involvement in the protoscolicidal action of rapamycin derivates and in calcium homeostasis. Int. J. Parasitol. 40, 651–661.

Cumino, A.C., Nicolao, M.C., Loos, J.A., Denegri, G., Elissondo, M.C., 2012. *Echinococcus granulosus* tegumental enzymes as *in vitro* markers of pharmacological damage: a biochemical and molecular approach. Parasitol. Int. 61, 579–585.

Di Sole, F., Vadnagara, K., Moe, O.W., Babich, V., 2012. Calcineurin homologous protein: a multifunctional Ca^{2+}-binding protein family. Am. J. Physiol. Renal Physiol. 303, F165.

Drews-Elger, K., Ortells, M.C., Rao, A., López-Rodriguez, C., Aramburu, J., 2009. The transcription factor NFAT5 is required for cyclin expression and cell cycle progression in cells exposed to hypertonic stress. PLoS ONE 4, e5245.

Fraga, D., Sehring, I.M., Kissmehl, R., Reiss, M., Gaines, R., Hinrichsen, R., Plattner, H., 2010. Protein phosphatase 2B (PP2B, calcineurin) in *Paramecium*: partial characterization reveals that two members of the unusually large catalytic subunit family have distinct roles in calcium-dependent processes. Eukaryot. Cell 9, 1049–1063.

Gajewski, K., Wang, J., Molkentin, J.D., Chen, E.H., Olson, E.N., Schulz, R.A., 2003. Requirement of the calcineurin subunit gene canB2 for indirect flight muscle formation in *Drosophila*. Proc. Natl. Acad. Sci. U. S. A. 100, 1040–1045.

Graef, I.A., Gastier, J.M., Francke, U., Crabtree, G.R., 2001. Evolutionary relationships among Rel domains indicate functional diversification by recombination. Proc. Natl. Acad. Sci. U. S. A. 98, 5740–5745.

Grybko, M.J., Bartnik, J.P., Wurth, G.A., Pores-Fernando, A.T., Zweifach, A., 2007. Calcineurin activation is only one calcium-dependent step in cytotoxic T lymphocyte granule exocytosis. J. Biol. Chem. 282, 18009–18017.

Høy, M., Bokvist, K., Xiao-Gang, W., Hansen, J., Juhl, K., Berggren, P.O., Buschard, K., Gromada, J., 2001. Phentolamine inhibits exocytosis of glucagon by Gi2 protein-dependent activation of calcineurin in rat pancreatic α-cells. J. Biol. Chem. 276, 924–930.

Hunter, T., 1995. Protein kinases and phosphatases: the yin and yang of protein phosphorylation and signaling. Cell 80, 225–236.

Hurd, H., Mackenzie, K.S., Chappell, L.H., 1993. Anthelmintic effects of cyclosporin A on protoscoleces and secondary hydatid cysts of *Echinococcus granulosus* in the mouse. Int. J. Parasitol. 23, 315–320.

Kilka, S., Erdmann, F., Migdoll, A., Fischer, G., Weiwad, M., 2009. The proline-rich N-terminal sequence of calcineurin A determines substrate binding. Biochemistry 48, 1900–1910.

Kim, M.J., Jo, D.G., Hong, G.S., Kim, B.J., Lai, M., Cho, D.H., Kim, K.W., Bandyopadhyay, A., Hong, Y.M., Kim, D.H., Cho, C., Liu, J.O., Snyder, S.H., Jung, Y.K., 2002. Calpain-dependent cleavage of cain/cabin1 activates calcineurin to mediate calcium-triggered cell death. Proc. Natl. Acad. Sci. U. S. A. 99, 9870–9875.

King, M.M., Huang, C.Y., 1984. The calmodulin-dependent activation and deactivation of the phosphoprotein phosphatase, calcineurin, and the effect of nucleotides, pyrophosphate, and divalent metal ions. J. Biol. Chem. 259, 8847–8856.

Klee, C.B., Ren, H., Wang, X., 1998. Regulation of the calmodulin-stimulated protein phosphatase, calcineurin. J. Biol. Chem. 273, 13367–13370.

Kujawski, S., Lin, W., Kitte, F., Börmel, M., Fuchs, S., Arulmozhivarman, G., Vogt, S., Theil, D., Zhang, Y., Antos, C.L., 2014. Calcineurin regulates coordinated outgrowth of zebrafish regenerating fins. Dev. Cell 28, 573–587.

Li, H., Rao, A., Hogan, P.G., 2011. Interaction of calcineurin with substrates and targeting proteins. Trends Cell Biol. 21, 91–103.

Li, S.Z., McDill, B.W., Kovach, P.A., Ding, L., Go, W.Y., Ho, S.N., Chen, F., 2007. Calcineurin-NFATc signaling pathway regulates AQP2 expression in response to calcium signals and osmotic stress. Am. J. Physiol. Cell Physiol. 292, 1606–1616.

Lin, X., Sikkink, R.A., Rusnak, F., Barber, D.L., 1999. Inhibition of calcineurin phosphatase activity by a calcineurin B homologous protein. J. Biol. Chem. 274, 36125–36131.

Liu, J., Farmer Jr., J.D., Lane, W.S., Friedman, J., Weissman, I., Schreiber, S.L., 1991. Calcineurin is a common target of cyclophilin–cyclosporin A and FKBP–FK506 complexes. Cell 66, 807–815.

McManus, D.P., Zhang, W., Li, J., Bartley, P.B., 2003. Echinococcosis. Lancet 362, 1295–1304.

Mecozzi, B., Rossi, A., Lazzaretti, P., Kady, M., Kaiser, S., Valle, C., Cioli, D., Klinkert, M.Q., 2000. Molecular cloning of *Schistosoma mansoni* calcineurin subunits and immunolocalization to the excretory system. Mol. Biochem. Parasitol. 110, 333–343.

Mellström, B., Savignac, M., Gomez-Villafuertes, R., Naranjo, J.R., 2008. Ca^{2+}-operated transcriptional networks: molecular mechanisms and in vivo models. Physiol. Rev. 88, 421–449.

Nicolao, M.C., Denegri, G.M., Cárcamo, J.G., Cumino, A.C., 2014a. P-glycoprotein expression and pharmacological modulation in larval stages of *Echinococcus granulosus*. Parasitol. Int. 63, 1–8.

Nicolao, M.C., Elissondo, M.C., Denegri, G.M., Goya, A.B., Cumino, A.C., 2014b. In vitro and in vivo effects of tamoxifen against larval stage *Echinococcus granulosus*. Antimicrob. Agents Chemother. 58, 5146–5154.

Oka, T., Dai, Y.S., Molkentin, J.D., 2005. Regulation of calcineurin through transcriptional induction of the calcineurin A promoter *in vitro* and *in vivo*. Mol. Cell. Biol. 25, 6649–6659.

Orrego, P.R., Olivares, H., Cordero, E.M., Bressan, A., Cortez, M., Sagua, H., Neira, I., González, J., da Silveira, J.F., Yoshida, N., Araya, J.E., 2014. A cytoplasmic new catalytic subunit of calcineurin in *Trypanosoma cruzi* and its molecular and functional characterization. PLoS Neglect. Trop. Dis. 8, e2676.

Pang, Z.P., Südhof, T.C., 2010. Cell biology of Ca^{2+}-triggered exocytosis. Curr. Opin. Cell Biol. 22, 496–505.

Perrino, B.A., Wilson, A.J., Ellison, P., Clapp, L.H., 2002. Substrate selectivity and sensitivity to inhibition by FK506 and cyclosporin A of calcineurin heterodimers composed of the R or catalytic subunit. Eur. J. Biochem. 269, 3540–3548.

Rascher, C., Pahl, A., Pecht, A., Brune, K., Solbach, W., Bang, H., 1998. Leishmania major parasites express cyclophilin isoforms with an unusual interaction with calcineurin. Biochem. J. 334, 659–667.

Raufman, J.P., Malhotra, R., Raffaniello, R.D., 1997. Regulation of calcium-induced exocytosis from gastric chief cells by protein phosphatase-2B (calcineurin). Biochim. Biophys. Acta 1357, 73–80.

Roberts, H.C., Sternberg, J.M., Chappell, L.H., 1997. Characterization of calcineurin from *Hymenolepis microstoma* and *H. diminuta* and its interaction with cyclosporin A. Parasitology 114, 279–283.

Rodríguez, A., Roy, J., Martínez-Martínez, S., López-Maderuelo, M.D., Niño-Moreno, P., Ortí, L., Pantoja-Uceda, D., Pineda-Lucena, A., Cyert, M.S., Redondo, J.M., 2009. A conserved docking surface on calcineurin mediates interaction with substrates and immunosuppressants. Mol. Cell, 616–626.

Rogan, M.T., Richards, K.S., 1986. *Echinococcus granulosus*: *in vitro* effect of monensin on the tegument of the protoscolex. Parasitology 93, 347–355.

Rusnak, F., Mertz, P., 2000. Calcineurin: form and function. Physiol. Rev. 80, 1483–1522.

Schulz, R.A., Yutzey, K.E., 2004. Calcineurin signaling and NFAT activation in cardiovascular and skeletal muscle development. Dev. Biol. 266, 1–16.

Semsarian, C., Wu, M.J., Ju, Y.K., Marciniec, T., Yeoh, T., Allen, D.G., Harvey, R.P., Graham, R.M., 1999. Skeletal muscle hypertrophy is mediated by a Ca^{2+}-dependent calcineurin signalling pathway. Nature 400, 576–581.

Shioda, N., Moriguchi, S., Shirasaki, Y., Fukunaga, K., 2006. Generation of constitutively active calcineurin by calpain contributes to delayed neuronal death following mouse brain ischemia. J. Neurochem. 98, 310–320.

Sim, A., Baldwin, M., Rostas, J., Holst, J., Ludowyke, R., 2003. The role of serine/threonine protein phosphatases in exocytosis. Biochem. J. 373, 641–659.

Singh, S., More, K.R., Chitnis, C.E., 2014. Role of calcineurin and actin dynamics in regulated secretion of microneme proteins in *Plasmodium falciparum* merozoites during erythrocyte invasion. Cell. Microbiol. 16, 50–63.

Srinivasan, S., Koenigstein, A., Joseph, J., Sun, L., Kalyanaraman, B., Zaidi, M., Avadhani, N.G., 2010. Role of mitochondrial reactive oxygen species in osteoclast differentiation. Ann. N. Y. Acad. Sci. 1192, 245–252.

Trama, J., Lu, Q., Hawley, R.G., Ho, S.N., 2000. The NFAT-related protein NFATL1 (TonEBP/NFAT5) is induced upon T cell activation in a calcineurin-dependent manner. J. Immunol. 165, 4884–4894.

Tsai, I.J., Zarowiecki, M., Holroyd, N., Garciarrubio, A., Sanchez-Flores, A., Brooks, K.L., Tracey, A., Bobes, R.J., Fragoso, G., Sciutto, E., Aslett, M., Beasley, H., Bennett, H.M., Cai, J., Camicia, F., Clark, R., Cucher, M., De Silva, N., Day, T.A., Deplazes, P., Estrada, K., Fernández, C., Holland, P.W., Hou, J., Hu, S., Huckvale, T., Hung, S.S., Kamenetzky, L., Keane, J.A., Kiss, F., Koziol, U., Lambert, O., Liu, K., Luo, X., Luo, Y., Macchiaroli, N., Nichol, S., Paps, J., Parkinson, J., Pouchkina-Stantcheva, N., Riddiford, N., Rosenzvit, M., Salinas, G., Wasmuth, J.D., Zamanian, M., Zheng, Y., The Taenia solium Genome Consortium, Cai, X., Soberón, X., Olson, P.D., Laclette,

J.P., Brehm, K., Berriman, M., 2013. The genomes of four tapeworm species reveal adaptations to parasitism. Nature 496, 57–63.
Tonks, N.K., Diltz, C.D., Fischer, E.H., 1988. Purification of the major protein tyrosine-phosphatases of human placenta. J. Biol. Chem. 263, 6722–6730.
Wu, H., Peisley, A., Graef, I.A., Crabtree, G.R., 2007. NFAT signaling and the invention of vertebrates. Trends Cell Biol. 17, 251–260.
Zheng, H., Zhang, W., Zhang, L., Zhang, Z., Li, J., Lu, G., Zhu, Y., Wang, Y., Huang, Y., Liu, J., Kang, H., Chen, J., Wang, L., Chen, A., Yu, S., Gao, Z., Jin, L., Gu, W., Wang, Z., Zhao, L., Shi, B., Wen, H., Lin, R., Jones, M.K., Brejova, B., Vinar, T., Zhao, G., McManus, D.P., Chen, Z., Zhou, Y., Wang, S., 2013. The genome of the hydatid tapeworm *Echinococcus granulosus*. Nat. Genet. 45, 1168–1175.